Earth and Planetary Science Letters 426 (2015) 13–22

Contents lists available at ScienceDirect

Earth and Planetary Science Letters

www.elsevier.com/locate/epsl

PdS receiver function evidence for crustal scale thrusting, relic subduction, and mafic underplating in the Trans-Hudson Orogen and Yavapai province

S. Thurner*, R. Margolis, A. Levander, F. Niu

Department of Earth Science, Rice University, Houston, TX, USA

ARTICLE INFO

Article history:
Received 12 September 2014
Received in revised form 29 May 2015
Accepted 2 June 2015
Available online 18 June 2015
Editor: P. Shearer

Keywords:
receiver functions
Trans-Hudson orogen
mafic underplating
relic subduction

ABSTRACT

The Trans-Hudson Orogen (THO) in the north central United States represents a major suturing event between the Wyoming and Superior Archean provinces. It is bounded to the south by the NE–SW striking Yavapai province, which was accreted along the southeastern margin of North America between 1.71 and 1.68 Ga and was one of a series of major collisional events responsible for the assembly of Laurentia. In this study, PdS teleseismic receiver functions were used to investigate the deep crustal structure associated with these collisions. Using data from over 800 broadband seismic stations distributed throughout the Great Plains/Midcontinent region, we calculated 0.5 Hz receiver functions using 245 M > 6.0 teleseismic events. The receiver functions were then CCP (common conversion point) stacked to create a 3D image volume. Profiles through this image volume show evidence of crustal scale thrusting of the Wyoming province in the west over the Superior province in the east and a relic subduction zone associated with the Yavapai–Superior boundary. We also performed a density analysis of the region using relative amplitude of the 2p1s and 0p1s receiver function phases from 233 stations. These data indicate a relatively low Moho density contrast throughout the THO and northern Yavapai Province associated with a region of thickened crust (>50 km), which we interpret to be evidence of a dense lower crustal layer that is the result of mafic underplating.

© 2015 Elsevier B.V. All rights reserved.

1. Introduction

The Trans-Hudson Orogen (THO) is a Paleoproterozoic collisional belt that extends from the Hudson Bay through the Canadian provinces of Manitoba and Saskatchewan and south into the U.S. through western Montana and North and South Dakota (Fig. 1a). This orogen developed during the formation of the North American cratonic core between 2.0 and 1.8 Ga by a series of plate collisions between Archean continents (Whitmeyer and Karlstrom, 2007). The Trans-Hudson Orogen contains juvenile Paleoproterozoic terranes caught within these collisions as well as the reworked Archean margins of the Superior, Hearne, and Wyoming provinces, which bound the THO to the east, northwest, and southwest respectively. The Trans-Hudson Orogen is bounded to the south by the Yavapai Province primarily comprised of juvenile arc crust, which was accreted along the southeastern margin of North America between 1.71 and 1.68 Ga (Whitmeyer and Karlstrom, 2007). This accretion event, known as the Yavapai Orogeny, was one in a series of accretion events that progressively built the North American continent to the southeast between 1.84 and 0.95 Ga (Hoffman, 1988; Whitmeyer and Karlstrom, 2007).

The THO, comparable to the modern Himalayas in scale (Whitmeyer and Karlstrom, 2007), was an integral part of the tectonic evolution of North America. The modern lithospheric structure of this region, largely unaffected by subsequent tectonism, provides insight into the formation of a stable craton as well as Proterozoic plate tectonics. For these reasons, the Canadian Trans-Hudson Orogen was extensively studied during the Lithoprobe program, which consisted of numerous seismic reflection and wide-angle seismic surveys (Hajnal et al., 1997; Nemeth and Hajnal, 1998; Corrigan et al., 2005; Nemeth et al., 2005; White et al., 2005). The U.S. component of the orogen, however, has not received as much attention, in part due to the lack of basement exposure within the U.S. where outcrops are restricted to the Black Hills (Dahl et al., 1999). Latham et al. (1988), Klasner and King (1990), Nelson et al. (1993) and Baird et al. (1996) have all discussed results from a series of COCORP seismic reflection profiles crossing the Trans-Hudson Orogen just south of the U.S.–Canada border. Recent and more extensive investigations of this region, however, do not exist. There have been, however,

* Corresponding author. Tel.: +1 713 348 5169.
E-mail address: smt4@rice.edu (S. Thurner).

http://dx.doi.org/10.1016/j.epsl.2015.06.007
0012-821X/© 2015 Elsevier B.V. All rights reserved.

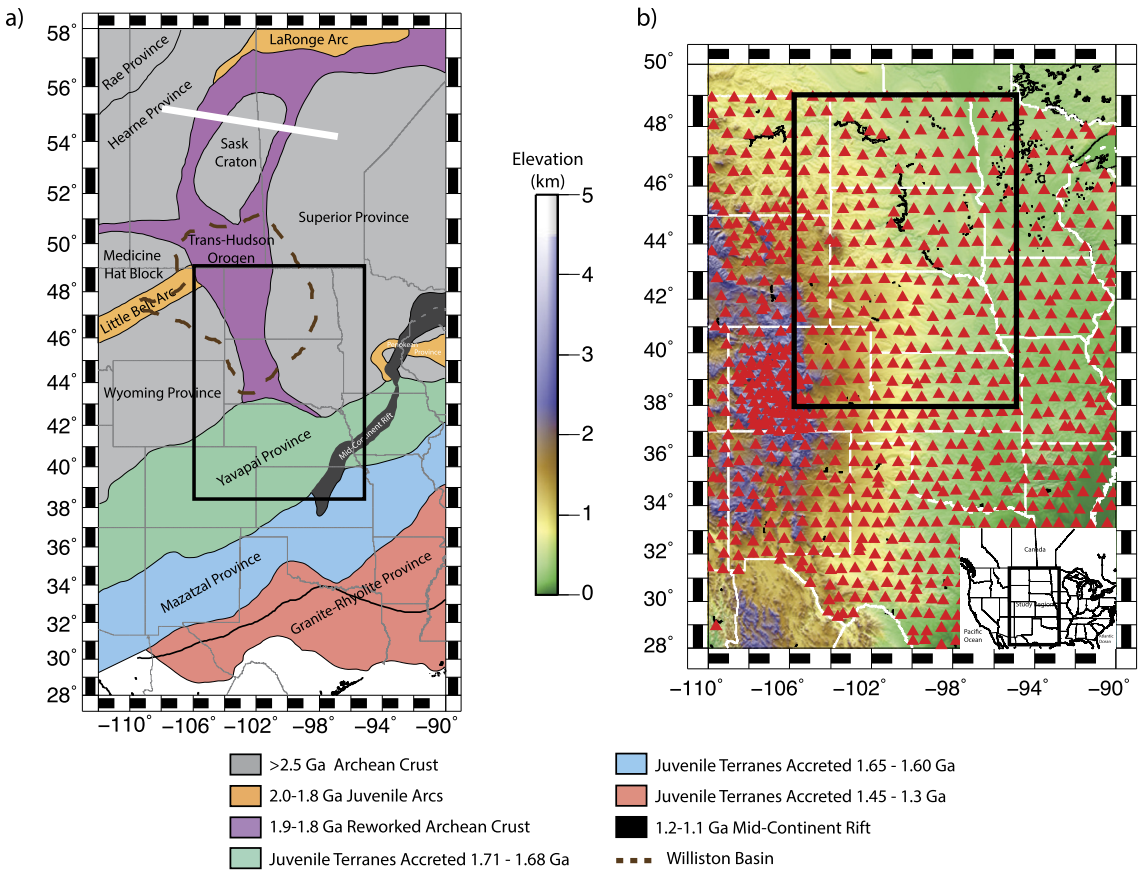

Fig. 1. a) Geologic map showing the distribution of geologic terranes associated with the formation of the North American continent. The black square indicates the focused study region; the white bold line marks the location of the Lithoprobe profile across the Trans-Hudson Orogen. b) Topography and station distribution map showing the location of all broadband stations for which receiver functions were calculated.

numerous studies to the west of the U.S. Trans-Hudson Orogen including the COCORP, Deep Probe, and CD-ROM experiments, which reveal visible subduction zone scars across the WY–Proterozoic boundary (Cheyenne Belt) (Yuan and Dueker, 2005), an indistinct Moho west of the Trans-Hudson Orogen (Allmendinger, 1982; Brown et al., 1983; Braile, 1989; Nelson et al., 1993; Baird et al., 1996), possibly resulting from a gradational phase change (Smithson, 1989), and a high velocity lower crustal layer within the Wyoming province, which may be the result of Proterozoic underplating and metamorphism of the Archean crust (Braile, 1989; Clowes et al., 2002; Gorman et al., 2002; Snelson et al., 2005; Karlstrom et al., 2005).

Using data from the USArray Transportable Array, we present a PdS receiver function analysis of the crustal structure throughout the central U.S. including the southern extension of the Trans-Hudson Orogen and the Proterozoic accreted terranes to the south. At 70 km station spacing this network does not provide complete coverage of the Moho, as PdS Fresnel zones (∼10–20 km) do not overlap at Moho depths, but is nonetheless a good opportunity to image the deep crustal structure associated with continental suturing processes.

2. Geologic setting

The northern Trans-Hudson Orogen is a suture between the Archean Hearne Province and the Archean Superior Province, which collided after the closure of the intervening Manikewan Ocean (Hammer et al., 2010). Ocean closure began ∼1.92 Ga and the resulting subduction initiated the formation of island arc and ophiolite complexes within the ocean basin, which were accreted onto the Hearne passive margin by both west and east dipping subduction processes (Corrigan et al., 2005). By ∼1.835 Ga the northward moving Sask craton, a much smaller Archean continent, collided with the Hearne craton and the accreted terranes along its margin (Hammer et al., 2010). The advancement of the Superior craton to the east closed the remaining ocean basin and the terminal collision between the Hearne craton, the Superior craton, and the accreted terranes in between was complete by 1.65 Ga (Corrigan et al., 2005; Hammer et al., 2010).

The southern Trans-Hudson Orogen is a suture between the Archean Wyoming Province and the Superior Province. This collision began ∼1.77–1.715 Ga, 50–60 Myr after the northern collision (Dahl et al., 1999). Unlike in the northern extension of the Trans-Hudson Orogen, there is little isotopic evidence for early Proterozoic juvenile volcanic terranes within the southern segment, as drill core information suggests a crust dominated by Archean age granulitic material (Baird et al., 1996). Some terrains in the southern portion, however, do resemble those in the north, including the reworked Archean margins (Klasner and King, 1990). Additionally, some studies have suggested the presence of an Archean micro-continent, similar to the Sask craton found in the northern segment (Klasner and King, 1990; Baird et al., 1996).

Following the formation of the Trans-Hudson Orogen, the North American craton, Laurentia, continued to grow through a series of accretion events occurring between ∼1.8 and .95 Ga along the southeastern margin, forming the north-east trending Yavapai, Mazatzal, Granite-Rhyolite, and Grenville provinces. Both the Yavapai and Mazatzal accretion events were accompanied by the intrusion of granitoids, which served to “stitch” these terranes to the older crust to the north (Whitmeyer and Karlstrom, 2007). Additionally, there was a major magmatic phase ∼1.4 Ga, which

Keller et al. (2005) suggest resulted in the thickening of the crust to ∼45 km through the production of a mafic restite layer.

3. Data and methods

3.1. Data

The USArray Transportable Array is a regular grid of temporary broadband seismic stations being deployed across the United States with ∼70 km station spacing. Beginning in 2004, ∼400 stations were installed along the west coast. With a residence time of ∼2 yr, these stations were gradually moved west to east across the United States, and by 2013 have covered the entire contiguous United States. For this study, we collected data from ∼800 broadband seismic stations located within the Great Plains and Midcontinent region between −110° and −90° longitude (Fig. 1b). The majority of these stations were a part of the USArray TA deployment. However, we supplemented this dataset with data from four other networks in the region: the US permanent network, the New Madrid seismic network, the Oklahoma seismic network, and the Indiana University seismic network. We calculated PdS receiver functions for 245 magnitude greater than 6.0 events located between 30° and 90° from each station. We also analyzed Bouguer gravity data from the study region. These data were collected from the Gravity Database of the U.S. operated by the Pan-American Center for Earth and Environmental Studies (PACES).

3.2. Methods

3.2.1. Receiver functions and CCP stacking

A receiver function (RF) is a time series computed from a three-component seismogram, with arrivals corresponding to P-wave to S-wave (PdS) conversions generated by discontinuities in the earth beneath a station. It is an approximation of the S wave Green's function resulting from S conversions from an incident teleseismic P wave (Bostock, 2004; Rondenay, 2009). The positive amplitude arrivals correspond to an increase in seismic impedance with depth (e.g., Moho) and negative amplitudes correspond to a decrease in seismic impedance with depth (e.g., lithosphere–asthenosphere boundary, LAB) (Langston, 1979; Ammon, 1991). This earth structure response can be isolated from the source and instrument response on a seismogram by deconvolving the vertical component from the horizontal component (radial and tangential). In this study, PdS RFs were calculated using both water-level frequency domain deconvolution (Burdick and Langston, 1977) and time-domain iterative deconvolution (Ligorría and Ammon, 1999). We show results from the Water Level method, which uses a simple division of the radial component by the vertical component in the frequency domain. However, noise can cause this division to become unstable when the vertical component spectrum reaches very small values. The Water Level method employs a type of stabilizing regularization in order to perform the division. A Gaussian filter is also used to control the width of the pulse and the high corner frequency of the resulting RF (Ammon, 1991).

We calculated receiver functions with a high corner frequency of 0.5 Hz assuming an average lower crustal *Vs* of ∼4 km/s and a vertical resolution of ∼0.25λ, this allows for the resolution of vertical structure at the ∼2 km scale. Note here that the Moho depth is defined as the midpoint depth corresponding to a boundary layer with a steep velocity gradient. The resolution is meant to be the uncertainties in our estimates of this depth rather than the resolvability on the thickness of the boundary layer, known as the sharpness of the interface.

All receiver functions were visually inspected and those with a low signal to noise ratio or otherwise flawed by dead traces or noise spikes were removed. In total, we were left with 41,737 high quality receiver functions, with an average of ∼50 traces for each station. The common conversion point stacking technique (Dueker and Sheehan, 1997) was then applied to the data using the depth conversion and lateral migration as outlined in Levander and Miller (2012). Using this method a 3-D image volume, spaced 0.25° × 0.25° laterally and 1 km vertically, was created and conversion horizons were picked directly from this volume. The receiver functions were converted to depth and repositioned into the 3D space where converted phases were sorted into CCP bins at each depth interval and subsequently summed. The depth conversion was performed using the IASP91 1-D velocity model modified with the Crust2.0 model at shallow depths (Bassin et al., 2000). Amplitudes were weighted and spread across the first Fresnel zone around each conversion point as described by Levander and Miller (2012). With station spacing of ∼70 km, the Fresnel zones at the crustal depths considered in this study (∼15–75 km) did not necessarily overlap. Therefore, in order to create continuous CCP profile images, the final stacked volume was further smoothed using a 2D Gaussian weighting filter.

3.2.2. Density analysis

Receiver functions are commonly used to determine Moho depth from the P to S converted phase, which is most often the dominant phase on a PdS receiver function. Crustal reverberations, however, can be combined with the P to S converted phase to better constrain Moho depth and *Vp*/*Vs* ratio (Zhu and Kanamori, 2000), as well as the density contrast associated with the crust-mantle boundary (Niu and James, 2002). In principle, the density contrast across the Moho can be estimated from the amplitudes of the Moho conversion and the reverberated phases. We employ the technique described by Niu and James (2002) to determine the relative density contrast at the Moho for stations distributed throughout the entire Great Plains/Midcontinent region. Receiver functions at each station were stacked using an *n*-th root stacking method with $n = 2$ (Muirhead and Datt, 1976). Depending on the Moho depth, the depth to other discontinuities beneath a station, and the signal to noise ratio, the reverberated phases may not always be easily identified on a receiver function. We, therefore, analyzed the receiver function stacks for each station, eliminating those with a poor signal to noise ratio and those without a clear 2p1s reverberated phase. We then calculated the ratio of the 2p1s reverberated phase amplitude and the 0p1s Moho amplitude at 233 stations where a clear 2p1s phase is observed. Niu and James (2002) applied this technique to high quality receiver-function data of a dense broadband array to constrain the absolute lower crustal density. While the study area of Niu and James (2002) has a very flat, sharp Moho the region discussed in this study is highly variable. Additionally, this region is not covered by such a dense broadband array as that discussed in Niu and James (2002). We thus decide not to invert Moho density contrast from the observed 2p1s/0p1s amplitude ratio. Instead, we use the 2p1s/0p1s amplitude ratio as a proxy for Moho density contrast and use its lateral variation to characterize the lower crustal density of subset regions throughout the study area.

3.2.3. Gravity modeling

Deep crustal and lithospheric density variations cause gravity anomalies with long to intermediate wavelengths: ∼500 km for lithospheric mantle thickness and density variations, and greater than ∼250 km for Moho depth and lower crustal density variations (Watts and Daly, 1981; Tiwari et al., 2013). Wavelength filtered gravity data can, therefore, provide valuable information about deep crustal and lithospheric structure. Additionally, the spectrum of potential field data has been used in previous studies to determine the source depth of gravity and magnetic anomalies (Fedi et al., 1997; Bilim, 2007; Tiwari et al., 2013). A spectral analysis of

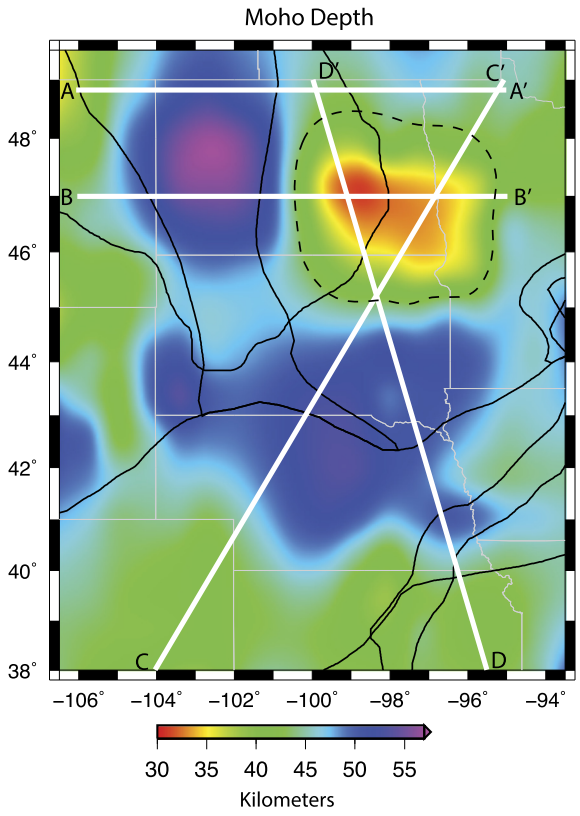

Fig. 2. Map showing Moho depth (km). The bold white lines show the locations of profiles shown in Figs. 3 and 4. The thin black lines represent the terrane boundaries as shown in Fig. 1. The black dashed line outlines the region discussed in Section 4.

the Bouguer gravity data in the Great Plains/Midcontinent study region reveals the deepest source depth to be ∼140 km, roughly coincident with lithosphere–asthenosphere boundary depth estimates from surface wave tomography results in the same region (Margolis, 2014). This source depth corresponds to a cut off gravity wave number of ∼.0025 km^{-1} and wavelength of ∼400 km. We filtered the Bouguer gravity data with a lowpass filter, resulting in gravity anomalies with wavelengths of ∼310 km that can be attributed to lower crust and uppermost mantle density and crustal thickness variations. We then used the GM-SYS Gravity/Magnetic Modeling Software to construct a 2D forward model of the filtered gravity data along a W–E profile across the Trans-Hudson Orogen at 47°N. We determined a 2D model to be sufficient for this study as most of the variation in the RF signals of interest occurs in the EW direction. The feature of interest is very consistent in the N–S direction, extending from ∼45° to 49°N (∼450 km).

4. Receiver function observations

After generating a 3D CCP image volume, the Moho depth was determined by averaging picks on latitude and longitude profiles throughout the region. The average Moho depth for the entire Great Plains/Midcontinent region is ∼45 km. The Moho depth map in Fig. 2, however, shows a much thicker crust (up to ∼55 km) beneath the Trans-Hudson Orogen and northern Yavapai boundary east of the Rocky Mountains. The area outlined by the dashed line in Fig. 2 represents a region where the Moho appears to shallow abruptly towards the east from ∼50 km to ∼30 km depth over ∼150 km distance. This abrupt shallowing of the Moho seems geologically unrealistic for a stable continental region that has not undergone tectonic deformation since the Precambrian. However, a clear Moho signal below 30 km cannot be identified in the receiver functions. This region also coincides with high Rayleigh wave phase velocities (20–25 s, Ge Jin, http://www.ldeo.columbia.edu/~ge.jin/projects/USarray.html) and high shear wave velocities determined from both Rayleigh wave and ambient noise tomography. These studies indicate positive *Vs* anomalies of ∼3–6% at 20–100 km depth (Margolis, 2014; Pollitz and Mooney, 2014), elevated *Vs* within the crust at ∼30–32 km depth, and *Vs* as high as 4.5 km/s at 38–40 km depth (Ryan Porter, personal communication).

4.1. Trans-Hudson Orogen

In order to determine the structure associated with the transition from the Trans-Hudson Orogen and the bounding Archean provinces, we examined latitude CCP profiles roughly perpendicular to the strike of the orogen. Fig. 3 shows two of these profiles at 48.75° and 47°N. In the northern profile (Fig. 3a) we see a strong positive (red) event at ∼37–41 km depth beneath the western Trans-Hudson Orogen. This Moho event is shallower than that seen on average throughout the Great Plains. However, it is consistent with both the COCORP seismic profile (Baird et al., 1996) and Pds and SdP receiver functions (Keenan et al., 2012), which show a relatively shallow Moho (∼40 km) in this same region. This Moho event deepens to ∼50 km beneath the central part of Trans-Hudson Orogen. Beginning at ∼102°W, we observe a second strong positive event within the crust, extending from ∼102° to ∼98°W and dipping east to west from ∼25 km depth to ∼50 km depth where it merges with the Moho signal. The deeper, Moho event is observed east of 101°W at ∼48–50 km depth beneath the Superior Province.

In order to verify whether the shallow positive event is truly associated with a P to S conversion characterized by a negative slowness, we computed the vespagram analysis for the shallow event by stacking the receiver functions along linear moveouts corresponding to a range of slownesses (e.g., Niu, 2014). We vary the slowness between −0.02 and 0.04 s/deg with an increment of 0.001 s/deg, which results in a total of 61 stacked receiver functions. The shallow event shows a slightly negative slowness (Fig. 3b), suggesting that it is likely a P to S converted phase.

Fig. 3c shows a CCP profile at latitude 47°N. Here we see a single positive event throughout the entire profile. This signal drastically decreases in depth in the center of the profile between 102° to 99°W where we observe the dipping event in the northern profile, suggesting that the two features are likely of the same origin. The vespagram analysis, on the other hand, shows that this event has a positive slowness (Fig. 3d), which is better explained by a reverberation phase from a shallow, horizontally lying structure. Since the event shown in Fig. 3c (black rectangle) is not perfectly horizontal, it is still possible that the anomalous slowness observed here is caused by the dipping.

4.2. Northern Yavapai boundary

We also examined the crustal structure associated with the boundary between the Yavapai province and the bounding Archean provinces to the north. Fig. 4 shows two diagonal profiles perpendicular to this boundary. In the first profile, oriented NE–SW, we see a strong Moho signal at ∼45 km depth to the northeast (Event A, Fig. 4a). This signal shallows to the southwest to ∼33 km depth in the central portion of the profile where we see two additional strong positive events, one shallow between ∼18 and 31 km depth dipping to the southwest (Event B, Fig. 4a), and one deep between ∼50 and 60 km depth dipping to the northeast (Event C, Fig. 4a). All of these signals are featured by a slightly negative slowness (Fig. 4c), although the slowness is slightly larger than the theoretical values, which are indicated by purple horizontal arrows in

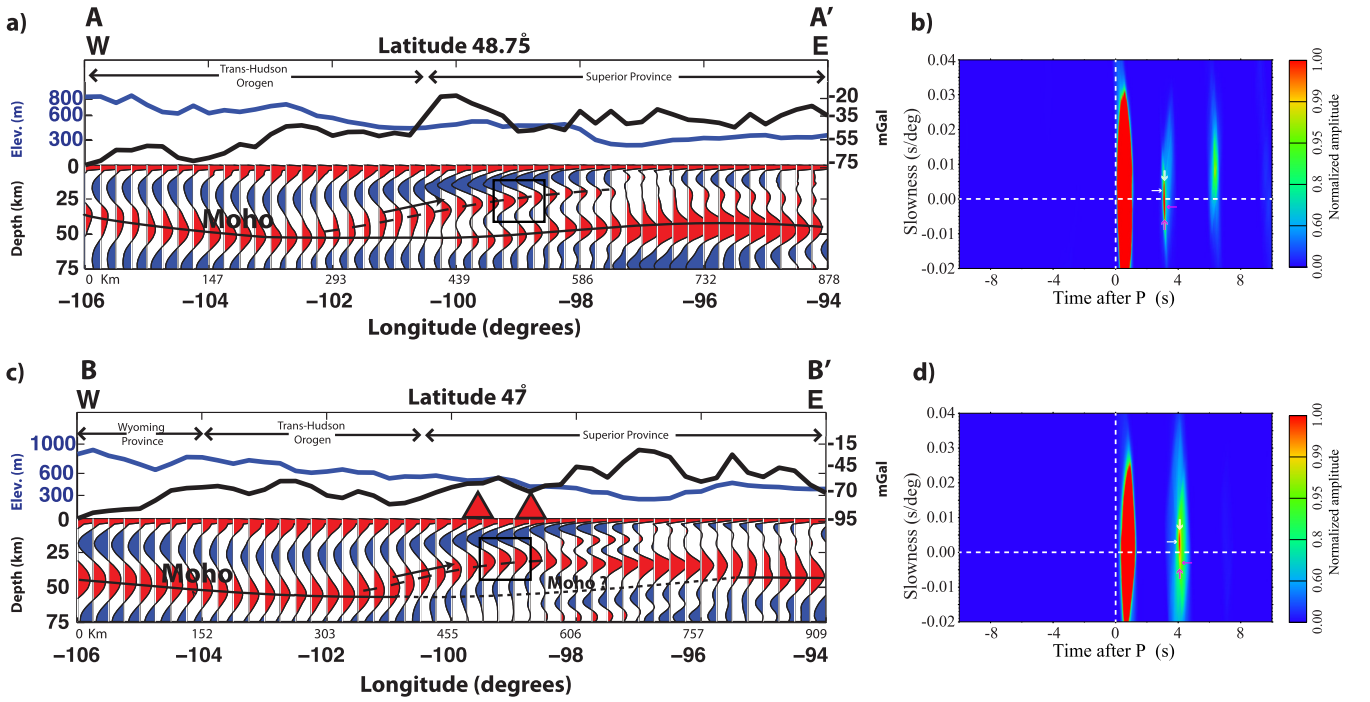

Fig. 3. Profiles through the CCP image volume showing crustal scale thrusting feature across the Trans-Hudson Orogen at 48.75°N (a) and 47°N (c). The blue lines indicate topography along each profile, the black lines indicate the Bouguer gravity anomaly along each profile, and the red triangles indicate stations with a low Moho density contrast as shown on the Moho map. (b) and (d) show the vespagrams of receiver functions binned at the locations shown by the black squares in each profile. These locations correspond to the receiver function event of interest discussed in the text. In each vespagram, the amplitude of the stacked receiver functions is plotted in color contour as a function of slowness and arrival time relative to the direct P arrival. Hotter color clusters represent greater energy and represent possible phase arrivals. Amplitude is normalized by the targeted later arrival, whose arrival time is indicated by the two vertical arrows. The white and purple horizontal arrows show the calculated relative slowness of a reverberation and a P-to-S converted phase with the same arrival time, respectively. (For interpretation of the references to color in this figure, the reader is referred to the web version of this article.)

Fig. 4c. Thus we tend to interpret them as the P to S converted phases instead of shallow multiples. In the southwestern portion of the profile we again see one positive Moho signal at ∼43 km depth (Event D, Fig. 4a).

We see a very similar structure in the second profile oriented NW–SE. There is a strong shallow signal in the northwest at ∼30 km depth (Event A, Fig. 4b). Again, in the central portion of the profile we see multiple positive events between ∼15 and 60 km depth (Events B and C, Fig. 4b) and a single Moho event in the southeast at ∼40 km depth (Event D, Fig. 4b).

5. Discussion

5.1. WY–Superior suture zone

We obtain crustal depth estimates ranging from ∼47–55 km beneath the Trans-Hudson Orogen. These estimates are slightly deeper than those based on COCORP reflection data by Baird et al. (1996) who propose a crustal model across the Trans-Hudson Orogen with Moho depths extending from ∼42 to 50 km depth. However, the deeper Moho depth estimates of this study are consistent with those from previous studies of the northern portion of the Trans-Hudson orogen. Hajnal et al. (1984), for example, report crustal thicknesses greater than 50 km from COCRUST refraction profiles just north of the U.S.–Canada border across the Williston Basin and Trans-Hudson Orogen. Results from the Lithoprobe project also indicate Moho depths greater than 50 km beneath the western portion of the Trans-Hudson Orogen (White et al., 2005; Hammer et al., 2010).

We interpret the dipping crustal events, seen in Fig. 3 as evidence of crustal scale overthrusting. Previous Lithoprobe and COCORP studies (Nelson et al., 1993; Baird et al., 1996; White et al., 2005; Hammer et al., 2010) also suggest crustal thrusting at the same scale. The Lithoprobe results to the north indicate an antiformal crustal culmination cored by the Sask micro-continent with strong reflections dipping beneath both bounding Archean cratons (Lewry et al., 1994). Nelson et al. (1993) and Baird et al. (1996) present similar results from a COCORP seismic reflection transect just south of the U.S.–Canada border. In this study, we observe strong, dipping signals in the crust consistent with thrusting of the Wyoming craton in the west over the Superior craton in the east.

It is likely that the strong, dipping crustal events represent the decollement or suture zone between the Superior craton and the overriding Wyoming craton. We suggest that this structure is analogous to the Kapuskasing uplift in the central Superior province. Thought to be a result of Trans-Hudson orogen compression, this structure consists of mid- to lower crustal rocks that have been brought to the surface (Percival and McGrath, 1986; Clowes et al., 1992; Cook and Varsek, 1994). Another analogous location may be in the Athabasca terrane to the north, in the western Churchill province of central Canada, where the lower crust of the Rae domain was thrust above the middle crustal rocks of the Hearne domain during the early stages of the Trans-Hudson Orogeny (Williams and Hanmer, 2006; Dummond et al., 2008).

5.2. Relict Yavapai subduction

We interpret the deep, positive event in Fig. 4 to be evidence of a relic subduction zone. This signal extends from Moho depth to >60 km and dips from south to north. This is indicative of north directed subduction of the Yavapai Province beneath the Superior Craton. We suggest that the deep positive event seen in Fig. 4 is analogous to a "Type III reflection pattern near the Moho" described by Cook (2002) as "reflections that can be traced from the lower crust to beneath the reflection Moho". A similar mantle signal can be seen in numerous studies,

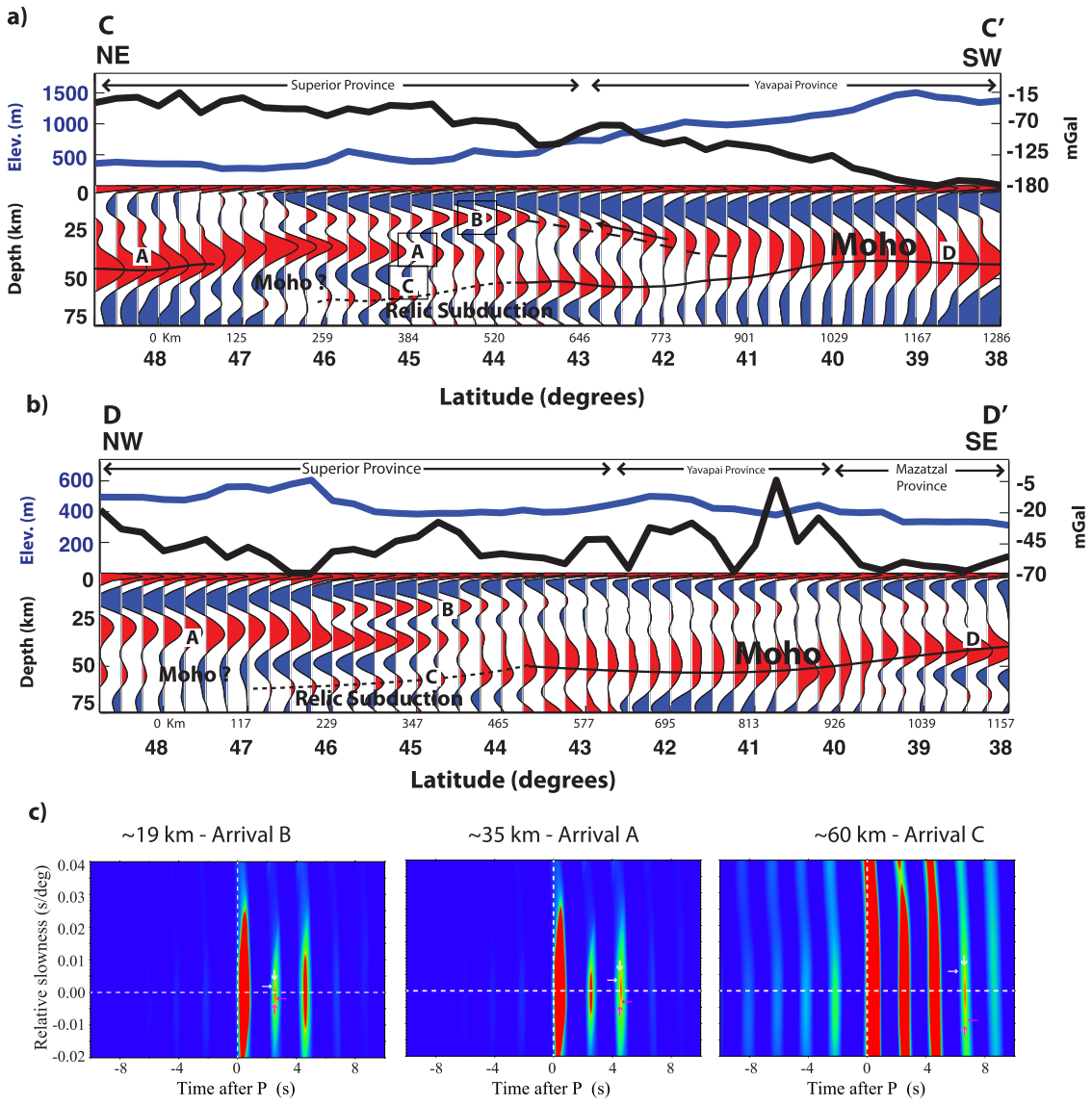

Fig. 4. NE–SW (a) and NW–SE (b) diagonal profiles through the CCP image volume showing evidence of relic subduction associated with Yavapai accretion. The dashed line indicates where obduction of the upper crust may have occurred and the dotted line indicates deep, subcrustal event that may be evidence of relic subduction and structural underplating of oceanic crust. The bold letters indicate the events discussed in Section 4.2 of the text. (c) Vespagram analysis for each of these events shown in (a) suggests that they are likely P to S converted phases, as they have a slightly negative slowness relative to the direct P arrival, although the slowness is slightly larger than the theoretical values (purple horizontal arrows). Each vespagram is plotted similarly as Fig. 3c.

including the seismic reflection profiles of the Abitibi–Grenville segment of the Lithoprobe project, which crosses the Grenville front at the Kapuskasing structural zone (Calvert et al., 1995; Cook et al., 1999, 2010). Yuan and Dueker (2005) also present evidence for a high velocity, north dipping, ancient slab preserved beneath the Cheyenne belt along the southern boundary of the Wyoming Province. We suggest that this north directed Yavapai subduction zone was preserved as oceanic crust underthrust the Superior province and became partially eclogitized as described by Cook et al. (1999). The shallow positive arrival may be indicative of a crocodile structure where separation of the upper and lower crust occurs when the upper layer is obducted (Event B, Fig. 4) and the lower layer is subducted (Event C, Fig. 4) as seen in previous studies of oceanic arcs (Lizarralde et al., 2002; Nakanishi et al., 2009; Thybo and Artemieva, 2013). The island arc accretionary processes described in these studies appear to extend over large distances and are perhaps analogous to the accretion of island arc terranes during the closing of the Manikewan Ocean.

5.3. Gravity modeling and mafic underplating

Fig. 5 shows the results of the forward modeling of the long-intermediate wavelength filtered Bouguer gravity data where we assume an asthenospheric density of 3.25 g/cm^3 and a lithospheric mantle density of 3.30 g/cm^3. The lithosphere–asthenosphere boundary was taken from surface wave tomography results (Margolis, 2014). We are able to model the observed Bouguer gravity data (RMS Error = 0.276) using a lower crustal density of 2.95 g/cm^3 throughout the profile and a layer of 3.1 g/cm^3 below the shallow positive event in the central and eastern portion of the profile. The absence of a consistent positive signal at the base of this layer, suggests that the density increase throughout the layer is gradational in nature. Also shown on this profile, directly above the dense layer, are the locations of two stations for which a relatively low Moho density contrast value was measured using the 2p1s/0p1s amplitude ratio. The gravity modeled dense layer, low Moho density contrast, and the seemingly transparent lower crust occur in the same region where

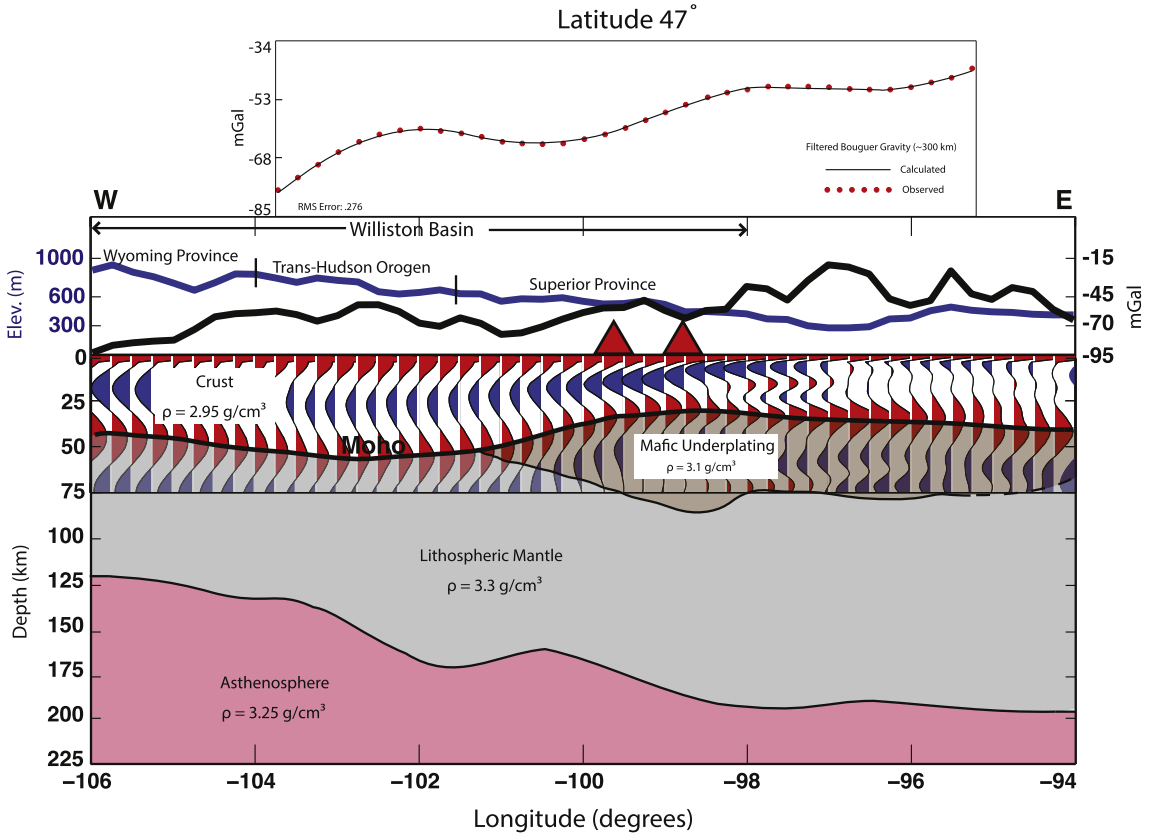

Fig. 5. Filtered Bouguer gravity anomaly and CCP profiles between 0 and 75 km depth. Along with density model used to forward model the intermediate (~300 km) wavelength Bouguer anomaly. The red dots indicate observed data and the black line indicates the forward modeled gravity anomaly. LAB depth taken from Margolis (2014). (For interpretation of the references to color in this figure legend, the reader is referred to the web version of this article.)

anomalously high S-wave velocities were found with ambient noise tomography (Ryan Porter, personal communication), providing compelling evidence for mafic underplating in this region. Thybo and Artemieva (2013) discuss similar crustal structures seen at other Precambrian suture zones including the tectonic boundary between the Hearne and Wyoming provinces, imaged in the Lithoprobe seismic refraction profile SAREX (Clowes et al., 2002; Gorman et al., 2002), and the boundary in the Baltic Shield between the Archean Karelian craton and the adjacent Proterozoic mobile belt. In both cases, dense, high velocity lower crustal layers have been attributed to Proterozoic magmatic underplating, which produced a dense lower crust consisting of a mixture of mafic granulites, pyroxenites, and eclogites (Kuusisto et al., 2006; Thybo and Artemieva, 2013). This is consistent with Durrheim and Mooney (1991, 1994) who find that Proterozoic crust (~40–55 km thick) is generally thicker than Archean crust (~27–40 km thick) and contains a much thicker high-velocity (>7.0 km/s) lower crustal layer, which they attribute to basaltic underplating facilitated by a decline in mantle temperatures in the Proterozoic.

5.4. Preservation of a dense lower crust

We calculated the 2p1s/0p1s amplitude ratio at 233 stations distributed throughout the study region (Fig. 6) and found an average ratio of .45. As described by Niu and James (2002), the 0p1s amplitude is almost solely determined by the Moho S-wave velocity contrast, while the 2p1s amplitude is sensitive to the Moho contrast of both the S velocity and density. Therefore the 2p1s/0p1s amplitude ratio serves as a proxy for Moho density contrast. We thus use these ratios to assess the relative Moho density contrast between various tectonic and geologic terranes throughout the region. In the Rocky Mountains we calculate an average ratio of .48, although we observe highly variable ratios throughout. This is consistent with a recently deformed region where crustal structure is highly variable over short distances. We calculate a similar average value of .46 in the Mazatzal and Granite–Rhyolite provinces, which have been relatively stable and undeformed since the Paleozoic. In the Rio Grande Rift, we observe a high average moho density contrast of .64, consistent with significant crustal thinning that has occurred in this region where a dense, high velocity lower crustal layer does not exist (Sinno et al., 1986). In contrast, we observe a relatively low ratio in the Yavapai province (.39) and an even lower ratio in the Archean terranes (.34). Additionally, we calculated the average 2p1s/0p1s amplitude ratio within the region of thickened crust shown in the Moho map (Fig. 2) and outlined in Fig. 6. Within this region we observe the lowest average ratio of .31, indicating a low density contrast at the Moho.

We, therefore, suggest the presence of a dense lower crustal layer throughout the Trans-Hudson region and the Yavapai province directly to the south. This layer may be the result of structural underplating and/or mafic underplating as described by Cook et al. (2010). The profiles in Fig. 4 suggest structural underplating associated with Yavapai accretion. In this case, subducted oceanic crust may have been emplaced below the continental crust during subduction and may have subsequently undergone partial eclogitization (Cook et al., 2010). However, it is also likely that magmatic underplating played a role in the formation of the dense lower crustal layer in the THO–Yavapai region. Accretion of the Proterozoic terranes along the southeastern margin of Laurentia was accompanied by plutonism and voluminous intrusion of granitoids (Whitmeyer and Karlstrom, 2007), which may have resulted in the emplacement of dense high-velocity basaltic intrusions into the crust as described by Keller et al. (2005). The relative abundance of this dense phase and the degree of eclogitization, however, may

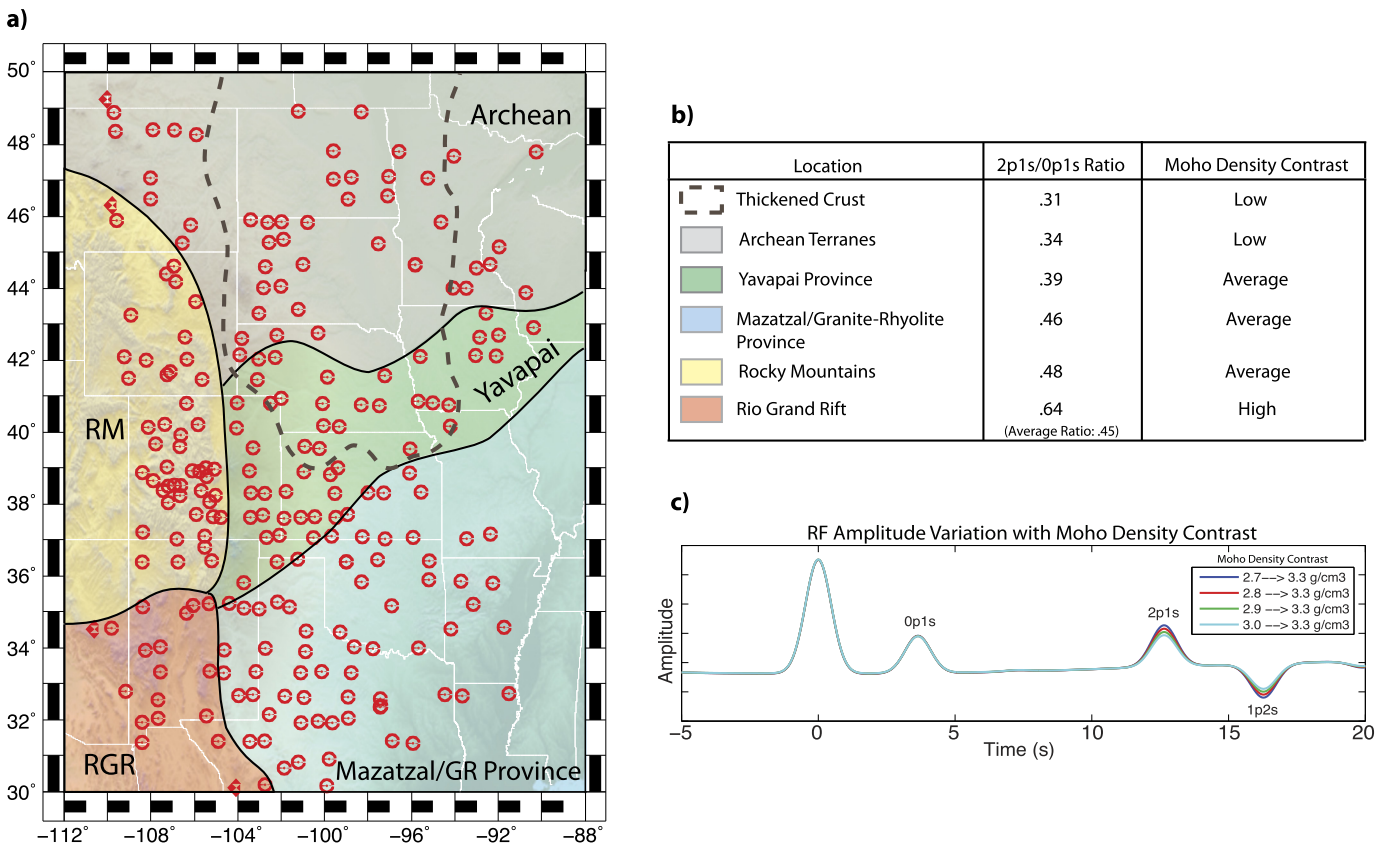

Fig. 6. (a) Map showing the stations used for the Moho density contrast calculation and the regions for which average ratios were calculated. RM = Rocky Mountains, RGR = Rio Grand Rift, GR = Granite–Rhyolite. (b) Table showing the 2p1s/0p1s amplitude ratio calculated for each region. (c) Synthetic receiver functions calculated for four separate velocity models with varying density contrast across the Moho. This figure shows the increased amplitude of the multiple phases corresponding to a higher density contrast across the Moho.

be variable throughout the region. We suggest the area with relatively thin crust to the east of the Trans-Hudson orogen underwent more complete eclogitization in order to account for the high shear wave velocities as well as the "unrealistic shallowing of the Moho", two characteristics which Mjelde et al. (2013) and Thybo and Artemieva (2013) present as evidence for the presence of mafic underplating and eclogitization. The 2p1s/0p1s amplitude ratios suggest mafic underplating over a large region including much of the Williston Basin, both the Wyoming and Superior Archean terranes, and a portion of the Yavapai province. We speculate that the widespread emplacement of such a dense lower crustal layer along with tectonic quiescence since the Precambrian played a role in the stabilization of this portion of the craton.

6. Conclusions

The Trans-Hudson orogen in the north central United States formed during a major suturing event between the Wyoming and Superior Archean provinces, and was one of the major collisional events responsible for the assembly of Laurentia. Receiver function CCP profiles show evidence of crustal scale thrusting of the Wyoming province in the west over the Superior province in the east. The THO is bounded to the south by the Yavapai province which was accreted to the southern boundary of the Archean provinces ~1.7 Ga. Profiles perpendicular to the strike of this boundary show evidence of structural underplating of what we interpret as oceanic crust, i.e. a frozen subduction zone. We also present evidence from receiver functions and gravity data suggesting the presence of a dense lower crustal layer throughout the Trans-Hudson region and Yavapai province. Density analysis using the relative amplitude of the 2p1s and 0p1s receiver function phases indicates a relatively low Moho density contrast throughout this area with respect to the surrounding Great Plains, Rocky Mountains, and Rio Grand Rift regions. These data suggest mafic underplating and the formation of a dense lower crust throughout the region, which may have contributed to the stabilization of this portion of the craton.

Acknowledgements

This research was partially funded by the U.S. National Science Foundation EAR-0844760 and the seismic data were collected from the IRIS DMC. Figures were made by GMT (Wessel and Smith, 1991). The authors would like to thank Ryan Porter for sharing his Ambient Noise Tomography results and Cin-Ty Lee, Julia Morgan, and Imma Palomeras for valuable discussion on structural and petrological interpretations. We also thank two anonymous reviewers for their constructive comments and suggestions, which significantly improved the quality of this paper.

Appendix A. Supplementary material

Supplementary material related to this article can be found online at http://dx.doi.org/10.1016/j.epsl.2015.06.007.

References

Allmendinger, R.W., 1982. COCORP profiling across the Rocky Mountain Front in southern Wyoming, Part 2: Precambrian basement structure and its influence on Laramide deformation. Geol. Soc. Am. Bull. 93, 1253–1263.
Ammon, C.J., 1991. The isolation of receiver effects from teleseismic P waveforms. Bull. Seismol. Soc. Am. 81 (6), 2504–2510.

Baird, D.J., Nelson, K.D., Knapp, J.H., Walters, J.J., Brown, L.D., 1996. Crustal structure and evolution of the Trans-Hudson orogen: results from seismic reflection profiling. Tectonics 15 (2), 416–426.
Bassin, C., Laske, G., Masters, G., 2000. The current limits of resolution for surface wave tomography in North America. Eos Trans. AGU 81 (F897).
Bilim, F., 2007. Investigations into the tectonic lineaments and thermal structure of Kutahya–Denizli region, western Anatolia, from using aeromagnetic, gravity and seismological data. Phys. Earth Planet. Inter. 165 (3), 135–146. http://dx.doi.org/10.1016/j.pepi.2007.08.007.
Bostock, M.G., 2004. Green's functions, source signatures, and the normalization of teleseismic wave fields. J. Geophys. Res. 109, B03303. http://dx.doi.org/10.1029/2003JB002783.
Braile, L.W., 1989. Crustal structure of the continental interior. In: Geological Society of America Memoirs, vol. 172, pp. 285–316.
Brown, L., Serpa, L., Setzer, T., Oliver, J., Kaufman, S., Lillie, R., Steeples, D.W., 1983. Intracrustal complexity in the United States midcontinent: preliminary results from COCORP surveys in northeastern Kansas. Geology 11 (1), 25–30.
Burdick, L.J., Langston, C.A., 1977. Modeling crustal structure through the use of converted phases in teleseismic body-wave forms. Bull. Seismol. Soc. Am. 67 (3), 677–691.
Calvert, A.J., Sawyer, E.W., Davis, W.J., Ludden, J.N., 1995. Archaean subduction inferred from seismic images of a mantle suture in the Superior Province. Nature 375, 670.
Clowes, R.M., Cook, F.A., Green, A.G., Keen, C.E., Ludden, J.N., Percival, J.A., West, G.F., 1992. Lithoprobe: new perspectives on crustal evolution. Can. J. Earth Sci. 29 (9), 1813–1864.
Clowes, R.M., Burianyk, M.J., Gorman, A.R., Kanasewich, E.R., 2002. Crustal velocity structure from SAREX, the southern Alberta refraction experiment. Can. J. Earth Sci. 39 (3), 351–373. http://dx.doi.org/10.1139/e01-070.
Cook, F.A., 2002. Fine structure of the continental reflection Moho. Geol. Soc. Am. Bull. 114 (1), 64–79.
Cook, F.A., Varsek, J.L., 1994. Orogen-scale decollements. Rev. Geophys. 32 (1), 37–60.
Cook, F.A., Velden, A.J., Hall, K.W., Roberts, B.J., 1999. Frozen subduction in Canada's Northwest Territories: lithoprobe deep lithospheric reflection profiling of the western Canadian Shield. Tectonics 18 (1), 1–24.
Cook, F.A., White, D.J., Jones, A.G., Eaton, D.W., Hall, J., Clowes, R.M., 2010. How the crust meets the mantle: lithoprobe perspectives on the Mohorovičić discontinuity and crust–mantle transition. Can. J. Earth Sci. 47 (4), 315–351. http://dx.doi.org/10.1139/E09-076.
Corrigan, D., Hajnal, Z., Németh, B., Lucas, S.B., 2005. Tectonic framework of a Paleoproterozoic arc-continent to continent–continent collisional zone, Trans-Hudson Orogen, from geological and seismic reflection studies. Can. J. Earth Sci. 42 (4), 421–434. http://dx.doi.org/10.1139/E05-025.
Dahl, P.S., Holm, D.K., Gardner, E.T., Hubacher, F.A., Foland, K.A., 1999. New constraints on the timing of Early Proterozoic tectonism in the Black Hills (South Dakota), with implications for docking of the Wyoming province with Laurentia. Geol. Soc. Am. Bull. 111 (9), 1335–1349. http://dx.doi.org/10.1130/0016-7606.
Dueker, K.G., Sheehan, A.F., 1997. Mantle discontinuity structure from midpoint stacks of converted P to S waves across the Yellowstone hotspot track. J. Geophys. Res., Solid Earth (1978–2012) 102 (B4), 8313–8327.
Dumond, G., McLean, N., Williams, M.L., Jercinovic, M.J., Bowring, S.A., 2008. High-resolution dating of granite petrogenesis and deformation in a lower crustal shear zone: Athabasca granulite terrane, western Canadian Shield. Chem. Geol. 254 (3), 175–196. http://dx.doi.org/10.1016/j.chemgeo.2008.04.014.
Durrheim, R.J., Mooney, W.D., 1991. Archean and Proterozoic crustal evolution: evidence from crustal seismology. Geology 19 (6), 606–609.
Durrheim, R.J., Mooney, W.D., 1994. Evolution of the Precambrian lithosphere: seismological and geochemical constraints. J. Geophys. Res., Solid Earth (1978–2012) 99 (B8), 15359–15374.
Fedi, M., Quarta, T., De Santis, A., 1997. Inherent power-law behavior of magnetic field power spectra from a Spector and Grant ensemble. Geophysics 62 (4), 1143–1150.
Gorman, A.R., Clowes, R.M., Ellis, R.M., Henstock, T.J., Spence, G.D., Keller, G.R., Miller, K.C., 2002. Deep Probe: imaging the roots of western North America. Can. J. Earth Sci. 39 (3), 375–398.
Hajnal, Z., Fowler, C.M.R., Mereu, R.F., Kanasewich, E.R., Cumming, G.L., Green, A.G., Mair, A., 1984. An initial analysis of the Earth's crust under the Williston Basin: 979 Cocrust experiment. J. Geophys. Res., Solid Earth (1978–2012) 89 (B11), 9381–9400.
Hajnal, Z., Nemeth, B., Clowes, R.M., Ellis, R.M., Spence, G.D., Burianyk, M.J.A., Forsyth, D.A., 1997. Mantle involvement in lithospheric collision: seismic evidence from the Trans-Hudson Orogen, western Canada. Geophys. Res. Lett. 24 (16), 2079–2082.s.
Hammer, P.T., Clowes, R.M., Cook, F.A., van der Velden, A.J., Vasudevan, K., 2010. The Lithoprobe trans-continental lithospheric cross sections: imaging the internal structure of the North American continent. Can. J. Earth Sci. 47 (5), 821–857.
Hoffman, P.F., 1988. United plates of America, the birth of a craton: Early Proterozoic assembly and growth of Laurentia. Annu. Rev. Earth Planet. Sci. 16, 543–603.
Karlstrom, K.E., Whitmeyer, S.J., Dueker, K., Williams, M.L., Bowring, S.A., Levander, A.R., et al., CD-ROM Working Group, 2005. Synthesis of results from the CD-Rom experiment: 4-D image of the lithosphere beneath the Rocky Mountains and implications for understanding the evolution of continental lithosphere. In: The Rocky Mountain Region: An Evolving Lithosphere Tectonics, Geochemistry, and Geophysics, pp. 421–441.
Keenan, J., Thurner, S., Levander, A., 2012. PdS receiver function imaging of the U.S. west of the Mississippi. In: AGU Fall Meeting 2012 Poster.
Keller, G.R., Karlstrom, K.E., Williams, M.L., Miller, K.C., Andronicos, C., Levander, A.R., Prodehl, C., 2005. The dynamic nature of the continental crust–mantle boundary: crustal evolution in the Southern Rocky Mountain region as an example. In: The Rocky Mountain Region: An Evolving Lithosphere Tectonics, Geochemistry, and Geophysics, pp. 403–420.
Klasner, J.S., King, E.R., 1990. A model for tectonic evolution of the Trans-Hudson orogen in North and South Dakota. The Early Proterozoic Trans-Hudson orogen of North America. In: Geological Association of Canada Special Paper, vol. 37, pp. 271–286.
Kuusisto, M., Kukkonen, I.T., Heikkinen, P., Pesonen, L.J., 2006. Lithological interpretation of crustal composition in the Fennoscandian Shield with seismic velocity data. Tectonophysics 420 (1), 283–299. http://dx.doi.org/10.1016/j.tecto.2006.01.014. Seismic.
Langston, C.A., 1979. Structure under Mount Rainier, Washington, inferred from teleseismic body waves. J. Geophys. Res., Solid Earth (1978–2012) 84 (B9), 4749–4762.
Latham, T.S., Best, J., Chaimov, T., Oliver, J., Brown, L., Kaufman, S., 1988. COCORP profiles from the Montana plains: the Archean cratonic crust and a lower crustal anomaly beneath the Williston basin. Geology 16 (12), 1073–1076.
Levander, A., Miller, M., 2012. Evolutionary aspects of lithosphere structure in the western U.S. Geochem. Geophys. Geosyst. 13, Q0AK07. http://dx.doi.org/10.1029/2012GC004056.
Lewry, J.F., Hajnal, Z., Green, A., Lucas, S.B., White, D., Stauffer, M.R., Clowes, R., 1994. Structure of a Paleoproterozoic continent–continent collision zone: a LITHOPROBE seismic reflection profile across the Trans-Hudson Orogen, Canada. Tectonophysics 232 (1), 143–160.
Ligorría, J.P., Ammon, C.J., 1999. Iterative deconvolution and receiver-function estimation. Bull. Seismol. Soc. Am. 89 (5), 1395–1400.
Lizarralde, D., Holbrook, W.S., McGeary, S., Bangs, N.L., Diebold, J.B., 2002. Crustal construction of a volcanic arc, wide-angle seismic results from the western Alaska Peninsula. J. Geophys. Res., Solid Earth (1978–2012) 107 (B8). EPM-4.
Margolis, R., 2014. Imaging the Great Plains of the Central U.S. using finite-frequency Rayleigh wave tomography and implications for asthenosphere-driven uplift. Masters thesis. Rice University.
Mjelde, R., Goncharov, A., Müller, R.D., 2013. The Moho: boundary above upper mantle peridotites or lower crustal eclogites? A global review and new interpretations for passive margins. Tectonophysics 609, 636–650. http://dx.doi.org/10.1016/j.tecto.2012.03.001.
Muirhead, K.J., Datt, R., 1976. The N-th root process applied to seismic array data. Geophys. J. Int. 47 (1), 197–210.
Nakanishi, A., Kurashimo, E., Tatsumi, Y., Yamaguchi, H., Miura, S., Kodaira, S., Hirata, N., 2009. Crustal evolution of the southwestern Kuril Arc, Hokkaido Japan, deduced from seismic velocity and geochemical structure. Tectonophysics 472 (1), 105–123. http://dx.doi.org/10.1016/j.tecto.2008.03.003.
Nelson, K.D., Baird, D.J., Walters, J.J., Hauck, M., Brown, L.D., Oliver, J.E., Sloss, L.L., 1993. Trans-Hudson orogen and Williston basin in Montana and North Dakota: new COCORP deep-profiling results. Geology 21 (5), 447–450. http://dx.doi.org/10.1130/0091-7613.
Németh, B., Clowes, R.M., Hajnal, Z., 2005. Lithospheric structure of the Trans-Hudson Orogen from seismic refraction-wide-angle reflection studies. Can. J. Earth Sci. 42 (4), 435–456. http://dx.doi.org/10.1139/E05-032.
Németh, B., Hajnal, Z., 1998. Structure of the lithospheric mantle beneath the Trans-Hudson Orogen, Canada. Tectonophysics 288 (1), 93–104.
Niu, F., 2014. Distinct compositional thin layers at mid-mantle depths beneath northeast China imaged by the USArray. Earth Planet. Sci. Lett. 402, 305–312. http://dx.doi.org/10.1016/j.epsl.2013.02.015.
Niu, F., James, D.E., 2002. Fine structure of the lowermost crust beneath the Kaapvaal craton and its implications for crustal formation and evolution. Earth Planet. Sci. Lett. 200 (1), 121–130.
Percival, J.A., McGrath, P.H., 1986. Deep crustal structure and tectonic history of the Northern Kapuskasing Uplift of Ontario: an integrated petrological–geophysical study. Tectonics 5 (4), 553–572.
Pollitz, F.F., Mooney, W.D., 2014. Seismic structure of the Central US crust and shallow upper mantle: uniqueness of the Reelfoot Rift. Earth Planet. Sci. Lett. 402, 157–166.
Rondenay, S., 2009. Upper mantle imaging with array recordings of converted and scattered teleseismic waves. Surv. Geophys. 204 (4–5), 377–405. http://dx.doi.org/10.1007/s10712-009-9071-5.
Sinno, Y.A., Daggett, P.H., Keller, G.R., Morgan, P., Harder, S.H., 1986. Crustal structure of the southern Rio Grande rift determined from seismic refraction profiling. J. Geophys. Res., Solid Earth (1978–2012) 91 (B6), 6143–6156.
Smithson, S.B., 1989. Contrasting types of lower crust. In: Properties and Processes of Earth's Lower Crust, pp. 53–63.
Snelson, C.M., Keller, G.R., Miller, K.C., Rumpel, H.M., Prodehl, C., 2005. Regional crustal structure derived from the CD-ROM 99 seismic refraction/wide-angle

reflection profile: the lower crust and upper mantle. In: The Rocky Mountain Region: An Evolving Lithosphere Tectonics, Geochemistry, and Geophysics, pp. 271–291.

Thybo, H., Artemieva, I.M., 2013. Moho and magmatic underplating in continental lithosphere. Tectonophysics 609, 605–619.

Tiwari, V.M., Ravi Kumar, M., Mishra, D.C., 2013. Long wavelength gravity anomalies over India: crustal and lithospheric structures and its flexure. J. Asian Earth Sci. 70, 169–178.

Watts, A.B., Daly, S.F., 1981. Long wavelength gravity and topography anomalies. Annu. Rev. Earth Planet. Sci. 9, 415–448.

White, D.J., Thomas, M.D., Jones, A.G., Hope, J., Németh, B., Hajnal, Z., 2005. Geophysical transect across a Paleoproterozoic continent–continent collision zone: the Trans-Hudson Orogen. Can. J. Earth Sci. 42 (4), 385–402. http://dx.doi.org/10.1139/E05-002.

Whitmeyer, S.J., Karlstrom, K.E., 2007. Tectonic model for the Proterozoic growth of North America. Geosphere 3 (4), 220–259. http://dx.doi.org/10.1130/GES00055.1.

Williams, M.L., Hanmer, S., 2006. Structural and Metamorphic Process in the Lower Crust: Evidence from a Deep-crustal Isobarically Cooled Terrane, Canada.

Yuan, H., Dueker, K., 2005. Upper mantle tomographic Vp and Vs images of the Rocky Mountains in Wyoming, Colorado, and New Mexico: evidence for a thick heterogenous lithosphere. In: Geophysical Monograph, vol. 154, p. 329.

Zhu, L., Kanamori, H., 2000. Moho depth variation in southern California from teleseismic receiver functions. J. Geophys. Res. 105, 2969–2980.